J Mater Sci: Mater Med (2010) 21:1867–1874
DOI 10.1007/s10856-010-4058-9

Fabrication of calcium phosphate–calcium sulfate injectable bone substitute using hydroxy-propyl-methyl-cellulose and citric acid

Van Viet Thai · Byong-Taek Lee

Received: 21 September 2009 / Accepted: 11 March 2010 / Published online: 24 March 2010

Abstract In this study, an injectable bone substitute (IBS) consisting of citric acid, chitosan, and hydroxyl propyl methyl cellulose (HPMC) as the liquid phase and tetra calcium phosphate (TTCP), dicalcium phosphate dihydrate (DCPD) and calcium sulfate dehydrate (CSD, $CaSO_4{\cdot}2H_2O$) powders as the solid phase, were fabricated. Two groups were classified based on the percent of citric acid in the liquid phase (20, 40 wt%). In each groups, the HPMC percentage was 0, 2, and 4 wt%. An increase in compressive strength due to changes in morphology was confirmed by scanning electron microscopy images. A good conversion rate of HAp at 20% citric acid was observed in the XRD profiles. In addition, HPMC was not obviously affected by apatite formation. However, both HPMC and citric acid increased the compressive strength of IBS. The maximum compressive strength for IBS was with 40% citric acid and 4% HPMC after 14 days of incubation in 100% humidity at 37°C.

1 Introduction

Hydroxyapatite (HAp) has been extensively used in clinical applications as a bone substitute and for bone augmentation. However, the clinical use of HAp as a bone substitute has been shown to be problematic. For instance, it has been difficult to prevent the dispersion of HAp granules and to mold the granules into the desired shape [1]. Composites, which consisted of one or more types of calcium phosphate, such as tetra calcium phosphate [TTCP, $Ca_4(PO_4)_2$], monocalcium phosphate monohydrate [MCPM, $Ca(H_2PO_4)_2{\cdot}H_2O$], β-tricalcium phosphate [β-TCP, $Ca_3(PO_4)_2$] and α-tricalcium phosphate (α-TCP), have been developed [2]. Brown and Chow reported on a calcium phosphate cement (CPC) that consists of TTCP and dicalcium phosphate dihydrate (DCPD, $CaHPO_4{\cdot}2H_2O$) or dicalcium phosphate anhydrous (DCPA, $CaHPO_4$) [1]. In addition, they demonstrated the formation of HAp by reacting TTCP with acidic calcium phosphate (DCPD or DCPA) [3].

Calcium phosphate cements (CPC) have attracted a lot of attention for their use in orthopaedic implants [4, 5]. However, CPC slowly resorbed into the apatite during the curing process. On the other hand, the resorption rate of calcium sulfate dehydrate (gypsum, CSD, $CaSO_4{\cdot}2H_2O$) was too fast to provide good support for new bone [4]. However, the addition of gypsum to the cement could overcome this drawback. Gypsum was previously shown to be relatively soluble in a calcium-rich phase [6]. In addition, when gypsum was used in conjunction with CSD, CSD was found to be eventually dissolved in vivo and the dissolved CSD reacted with the phosphate ions present in body fluids to form HAp crystals (or a mixture) [4, 6]. In a previous study, we fabricated calcium phosphate–calcium sulfate cements using calcium sulfate hemihydrate (CSH, $CaSO_4{\cdot}0.5H_2O$) and demonstrated that CSH increased the compressive strength of cements [7]. In this study, we used CSD instead of CSH to enhance the mechanical properties of cements.

The presence of additives was previously shown to affect various properties of CPC, such as the setting time, the porosity, and the mechanical behaviors [4, 5]. Citric acid ($C_6H_8O_7$) is an important intermediate product in the citric cycle in the metabolism of almost all living

V. V. Thai · B.-T. Lee (✉)
Department of Biomedical Engineering and Materials, School of Medicine, Soonchunhyang University, 366-1 Ssangyoung-Dong, 330-090 Cheonan, Republic of Korea
e-mail: lbt@sch.ac.kr

organisms. Since citric acid had a very high salting-out effect in the Hofmeister series and easily adsorbed inorganic precipitates, it had been proposed to enhance the strength of cement [8].

Chitosan, was a natural component of shrimps and crab shells, was shown to be biocompatible, biodegradable, nonantigenic, and nontoxic [7, 9]. Zhang and Zhang reinforced β-TCP composite scaffolds using chitosan and demonstrated that chitosan can greatly improve the mechanical properties of scaffolds [10].

Hydroxy propyl methyl cellulose (HPMC, $C_{56}H_{108}O_{30}$) was cellulose ether and that was derived from alkali treated cellulose that was reacted with methyl chloride and propylene oxide, one of the most commonly occurring polysaccharides [11]. Chappard et al. [12] evaluated the in vivo behaviour of an injectable bone substitute that contained HPMC as a polymer carrier. Cherng et al. [11] evaluated the effects of HPMC and chitosan on the properties of CPC when used in TTCP and DCPA. In this paper, it was hypothesized that mechanism behind the increased toughness of cements containing HPMC was the same as the mechanism seen in Portland cements.

Citric acid was expected to react with hydroxyl groups in HPMC and chitosan or with amino groups in chitosan to form ester cross-linking or an inter-ionic attraction. One of the characteristic properties of polysaccharides was their ability to form viscous solutions. Accordingly, citric acid could react with viscous HPMC and chitosan fibers in water, which formed a matrix of cages. This matrix could immobilize the CPC particles. For this reason, CPC could form a more orderly structure and increased the strength of materials.

The main goal of this investigation was to examine the influence of citric acid and HPMC on CPC properties. In each CPC group, which contained different citric acid concentrations, the effect of HPMC was evaluated in terms of initial setting time and compressive strength.

2 Experimental procedure

2.1 Materials

In this study, the cements consisted of a powder and liquid phase. The liquid component was a solution of chitosan, HPMC and citric acid in distilled water. The mass fraction of chitosan was set at 2 wt%. The two citric acid concentrations used were 20–40 wt%. Chitosan was purchased from Sigma (Iceland) and the degree of deacetylation was minimally 85%. Citric acid was purchased from Samchun Pure Chemical Co. Ltd (Pyongtaek, South of Korea). Hydroxy propyl methyl cellulose (HPMC) was purchased from Sigma-Aldrich. The mass of HPMC was measured and its mass percent in the distilled water of the liquid phase was 0, 2, and 4 wt%.

The powder component was a mixture of TTCP, DCPD, and CSD. The TTCP powder was synthesized using a solid-state method [3, 13]. The powders of TTCP, DCPD (Sigma, USA), and CSD (Samchun, South of Korea) were mixed in a ball grinder for 8 h in equimolar amounts (73.69 wt% of TTCP-like, 26.31 wt% of DCPD in total mass of two powders) to attain the CPC powder. The CSD constituent was fixed in the CPC powder at 20 wt%.

In this work, TTCP was synthesized according to Eq. (1), which was the common reaction used to produce TTCP [13]. The final TTCP was in the bulk form.

$$2CaHPO_4 + 2CaCO_3 \rightarrow Ca_4(PO_4)_2O + 2CO_2 + 3H_2O \quad (1)$$

The holding temperature was set at 1,500°C for 6 h. Burguera et al. investigated the effects of the overall calcium-to-phosphate (Ca/P) ratio of TTCP synthesis on the existence of impurities. They demonstrated that Ca/P ratios between 1.9 and 1.95 were safe approximations [14]. Therefore, the molar fractions of DCPA (Sigma, USA) and $CaCO_3$ (DC Chemical Co. Ltd) were 0.526–0.487, respectively.

TTCP and $CaCO_3$ powders were mixed and ground in a planetary ball grinder for 6 h. An anti-hygroscopic medium of anhydrous methyl alcohol was used because the particle sizes in the mixture were large enough to promote the reaction at high temperatures. For these reasons, the following sintering route was used: a heating rate of 5°C/min was used during heating and a cooling rate of 10°C/min was used during cooling. The cooling rate was similar to the quenching treatment since this approach will avoid the transformation of TTCP to phases that were more stable at lower temperature [14].

In this study, we investigated the six cement compositions shown in Table 1. The powder-to-liquid ratio was 1.8:1 [wt/wt]. The liquid and solid components were mixed manually with a spatula for 45 s or around 1 min until a chewing-gum-like slurry was achieved. The molding slurry was placed into tubes that were open on both sides. The diameter of the tubes was 9.5 mm, and the length of tubes was set such that the aspect ratio (length-to-diameter) was approximately 2.

2.2 Setting time measurement

The self-setting time of these cements was selected according to the ISO 9917 standard for dental silicophosphate cements [15]. The setting time of the samples was measured using a Gilmore needle test. All samples were considered set when a weight of 400 g was loaded onto the sample using a needle with a tip diameter of 1 mm

Table 1 Composition of the injectable bone substitutes

Sample name	Powder components [wt.%]		Liquid components [wt.%]			Incubation time [days]
	TTCP-DCPD	CSD	Chitosan	Citric acid	HPMC	
A20	80	20	2	20	0	1, 3, 7, 14
A40	80	20	2	40	0	1, 3, 7, 14
B20	80	20	2	20	2	1, 3, 7, 14
B40	80	20	2	40	2	1, 3, 7, 14
C20	80	20	2	20	4	1, 3, 7, 14
C40	80	20	2	40	4	1, 3, 7, 14

and no visible impression on the surface of the sample was observed in 100% relative humidity at 37°C.

2.3 Compressive strength measurement

The cements were molded into cylindrical columns. The samples were incubated in 100% relative humidity at 37°C for 1, 3, 7 and 14 days. At these time intervals the compressive strengths were measured using a computer controlled universal testing machine (R&B, Korea). The cross-head speed was 1 mm/min. For each measurement, an average of three samples was taken ($n = 5$).

2.4 X-ray diffraction analysis

The X-ray diffraction profiles (XRD, D/MAX-250, Rigaku, Tokyo, Japan) of different cements were recorded by X-ray powder diffraction analysis. CuKα radiation was used and generated at 40 kV and 200 mA. The diffraction angle was varied from 20 to 40° with a 2θ angle rate of 2 ^{0}/min.

2.5 Morphology observation of cements

The morphology of the cements was observed under scanning electron microscopy (SEM, JSM-635, JEOL, Tokyo, Japan) after setting and 14 days after the incubation process.

3 Results

3.1 Setting time

The cements were hardened through two processes. The initial process was hardening through the hydration of the salts in the powder component or/and chelate reactions between one or more constituents in the liquid component and powder component [1]. The second process was hardening through transformation of the composites of the cements to HAp [1, 6]. In this study, the setting time term referred to the initial process.

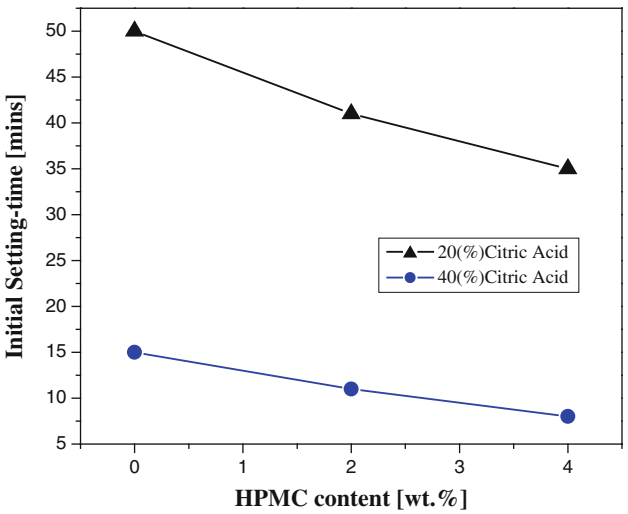

Fig. 1 Initial setting time versus percentage of citric acid and HPMC

In terms of HPMC content, the setting time decreased while the HPMC content increased from 0 to 4% in both G20 and G40 (Fig. 1). However, the setting times of G20 were always longer than those for G40 at the same HPMC mass rate. When evaluating the appropriateness of the setting time in regards to surgical time, G20 appeared to be better than G40. This was because the setting times of all G20 compositions were above 30 min, and those of G40 were short. Especially, for the setting time of C40, which was below 10 min. Therefore, G20 was typical IBS for curing of large bone defects such as clavicle bone defects; and G40 was typical IBS for curing of small bone defects such as finger bone defects.

The samples fabricated at three compositions were analyzed by the XRD method to determine the component substances, namely A20, C20, and C40, after they had finished setting to a hard state. The results are shown in Fig. 2. Based on this analysis, no new materials were observed, only the expected raw powders, TTCP, DCPD, and CSD. In the C40 composition, two HAp peaks appeared, but they were too weak to confirm a significant presence of HAp. The XRD data did not explain the setting time behavior of the three compositions examined. Therefore, the structure of the cements was further

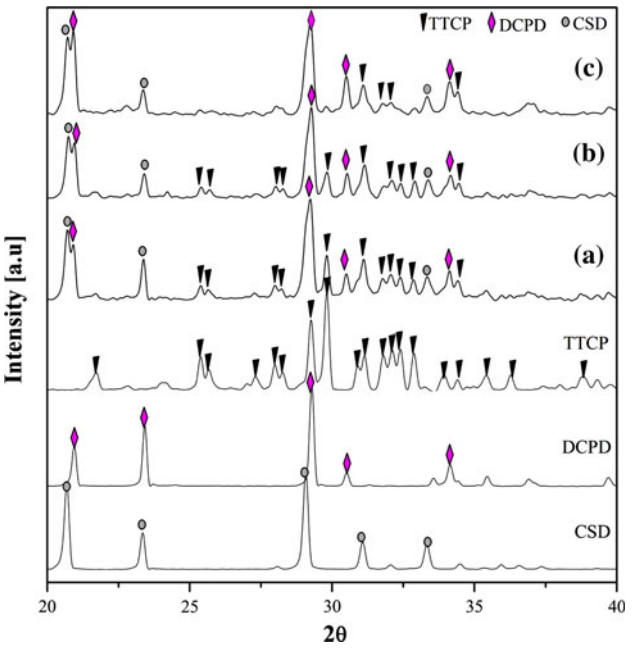

Fig. 2 Post-setting XRD profiles of (*a*) A20 (non-HPMC, 20 wt% citric acid), (*b*) C20 (4 wt% HPMC, 40 wt% citric acid), and (*c*) C40 (4 wt% HPMC, 40 wt% citric acid)

examined to better understand the setting time property. SEM images of the three compositions were shown in Fig. 3.

After the initial setting, the samples fabricated with the A20 composition consisted of an easily breakable thread. Their surface morphology could be used to interpret this phenomenon. Under micro-magnification, sub-micron particles were distributed around the main micron particles. These sub-micron particles were not uniformly distributed and they did not connect adjacent micron particles to each other (Fig. 3a,b).

Three types of morphologies were observed on the surfaces of both C20 and C40 (Fig. 3c,d,e,f). The type I morphology consisted of particles that had a rectangular shaped cross-section and the length of these particles were several micrometers. The type II morphology consisted of a micron porous area, where the pore diameters were almost below 1 μm. The type III morphology adopted a fibrous structure (Fig. 3e,f). The type I morphology occupied almost the entire surface area of the C20 samples and only a negligible area was occupied by the type II morphology and no surface morphology resembling type III was observed. However, a very small number of nano-sized particles could be found on the type I surfaces. The three types of morphologies were found on the surface of the C40 sample in various proportions. The area occupied by the type I structure was insignificant, where the area occupied by the type II morphology was the largest and these regions were surrounded by the type III structure. In the border between these two areas, nano-sized and fibrous particles were detected.

3.2 Compressive strength

The compressive strengths (Fig. 4) of the six cements increased with the time of incubation in 100% humidity at 37°C. The compressive strength of samples incubated for 0, 1, 3, 7, and 14 days was measured.

For all compositions, the compressive strengths monotonically increased as a function of incubation time. The compressive strength of the samples increased faster during the first 3 days than in the following days. For all

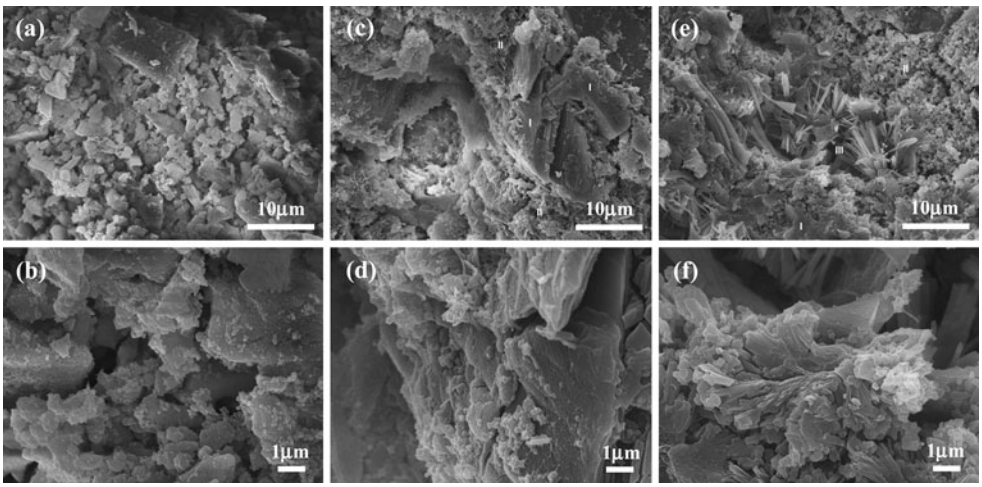

Fig. 3 SEM images of fracture surfaces of **a** A20 and **b** an enlarged image, **c** C20 and **d** an enlarged image, and **e** C40 and **f** an enlarged image after setting

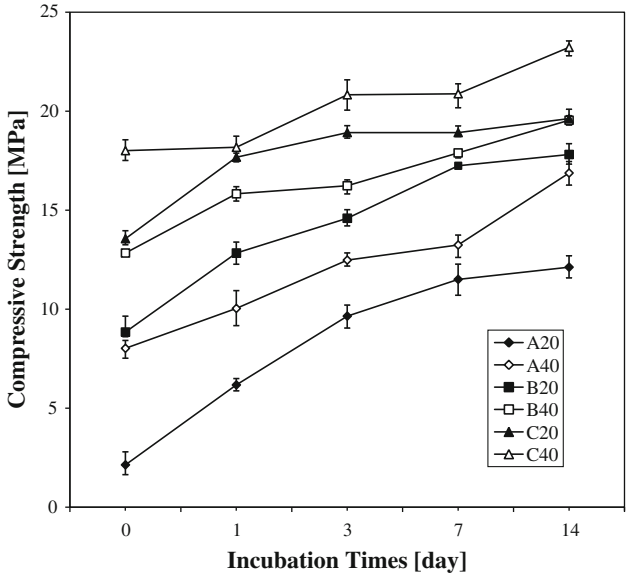

Fig. 4 Compressive strength versus days in air at 37°C and 100% humidity

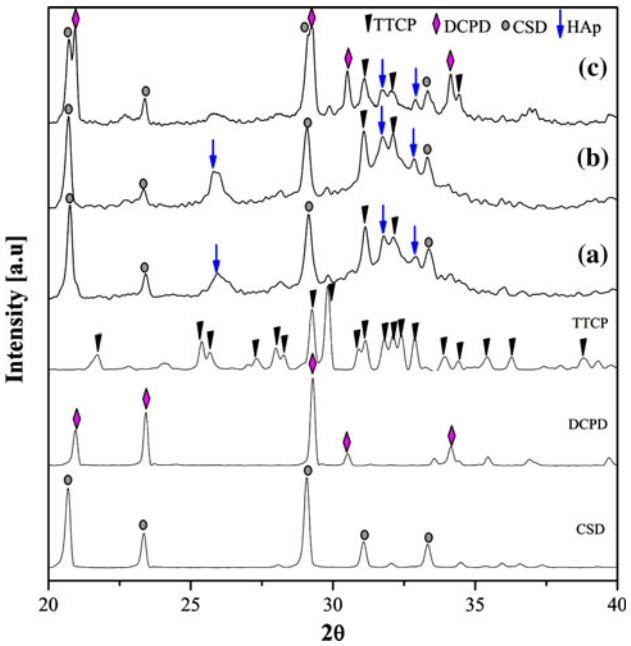

Fig. 5 XRD profiles of (*a*) A20, (*b*) C20, and (*c*) C40 after 14 days of incubation

compositions, the strength value was the highest after 14 days of incubation. The strength values of all compositions were greater than 15 MPa after 14 days of incubation except for A20 composition. In all groups the same trend was observed, longer incubation times resulted in increased HPMC content. Except for G20 at 0 day, the compressive strength of A20 was higher than that of C20, but the strength of both was relatively low and varied insignificantly. The differences became clear when G20 was compared to G40 at the same HPMC content. At the same HPMC content, the G40 composition was always stronger than the G20 composition. It was easy to distinguish these two groups, because the CS of G40 was 2 MPa higher than that of G20. Finally, the six compositions were considered concurrently. C40 was the hardest composition, and A20 was the weakest at all incubation times.

The hardness of any material depended on the essence of the components, the proportion of the components and their structure. Thus, XRD and SEM methods were performed to interpret the mechanical behavior of the cements. Figure 5 shows the XRD results of the three injectable bone substitutes, A20, C20, and C40, after incubation for 14 days.

The A20 composition was further evaluated because it had the lowest compressive strength. The C40 composition was chosen because it had the strongest compressive strength and the C20 composition was selected because it had the most suitable setting time and mechanical behavior for orthopedic surgery.

As shown in Fig. 5, the HAp peaks appeared in all three compositions. However, the HAp peaks in A20 and C20 profiles were larger than in the C40 profile. There were several HAp peaks in the XRD profiles of C40 that were weak; however, the raw materials were still obviously visible. In A20 and C20, the intensity of the HAp peaks was high and these peaks were almost at the main angles. Simultaneously, the major peaks corresponding to TTCP and DCPD almost completely vanished. This phenomenon could be explained easily by the reaction between TTCP and DCPD to form HAp. In addition, the CSD components remained intact at all three compositions. Bohner [6] previously suggested that when CSD eventually dissolves in vivo it reacts with phosphate ions present in body fluids to form HAp crystals. Therefore, CSD most likely remained in solution because of the absence of the HPO_4^{2-} ion in the incubated environment.

In the XRD spectra, components of the liquid phase were not shown. Therefore, SEM images were acquired to examine the role of the liquid phase. SEM images of the three compositions, A20, C20, and C40 after incubation for 14 days are displayed in Fig. 6. The morphology of these compositions was categorized by size and shape and three types were specified, namely, type I, type II and type III. The type I morphology was micron particles. Almost all the particles in the type I morphology had curved edges. The type II morphology consisted of a porous area containing pores that were about 1 μm in diameter. The type III morphology was characterized by a fibrous structure.

The A20 sample contained type I and type II morphologies at relatively similar ratios. However, they were not split clearly at the border, and they seemed to pile up at cliffs (Fig. 6b). This morphology did not appear in the C40 specimens and was only negligibly observed in C20 specimens. The surface of both C20 and C40 specimens

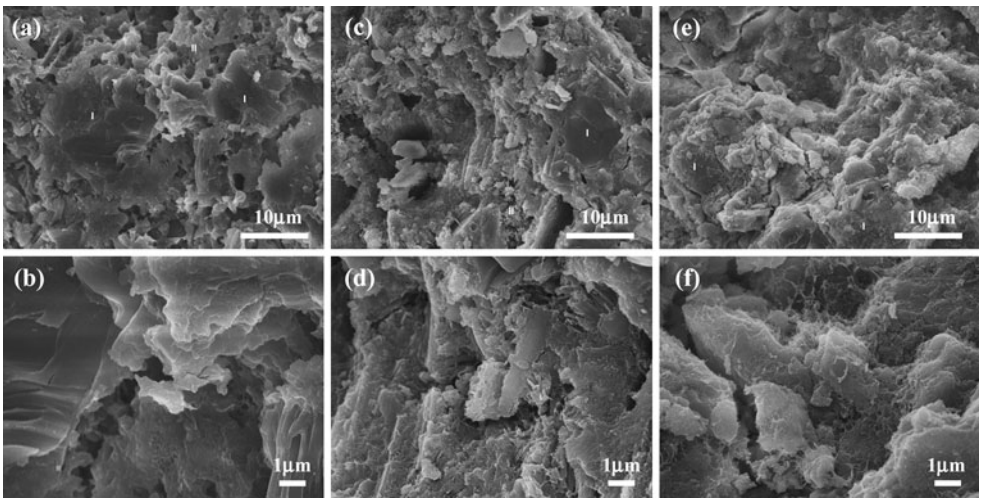

Fig. 6 SEM images of fracture surfaces of **a** A20 and **b** an enlarged image, **c** C20 and **d** an enlarged image, and **e** C40 and **f** an enlarged image after 14 days of incubation

was occupied by particles whose sizes were below 10 μm and these particles were surrounded by the type III morphology. However, these fibrous structures were smaller than the type III structures that were observed in the C40 specimens. In addition, they were also shaped individually. The type III morphology appeared to be denser in C40 than in C20.

4 Discussions

4.1 Effects of citric acid and HPMC on setting time of the cements

The liquid phase was required to make the IBS steadier and more homogeneous. Another function of the liquid phase was to act as the dispersive medium for the setting reactions (transformation to HAp) [1, 2, 6]. Thus, the liquid component made the setting reactions start earlier, hence the setting time decreased.

Fernández et al. [16] demonstrated the effect of citric acid on CPC, which acted as a water-reducing agent. In addition, citric acid molecules were shown to adsorb on the surfaces of powder nuclei. This adsorption was explained by the chelate reaction between citric acid and calcium in the powder component [1, 17] (chelation is the process of forming a ring by forming one or more hydrogen bonds). The powder particles, which absorbed citric acid molecules, conserved the amount of water molecules for hydration and increased the surface area available for dissolution. Hence, the precipitation of the powder component in the liquid component occurred earlier, which decreased the setting time. This mechanism readily explained the results attained in this study: the setting times of G40 were shorter than those of G20 at a similar HPMC content.

Dorozhkin [18] concluded that there were no reactions between HPMC and other inorganic matter. Therefore, in this study, HPMC was unable to react with any ceramics. One of the characteristic properties of polysaccharides is their ability to form viscous solutions. Visually, the liquid component with 4 wt% HPMC was in a gelatinous form, whereas the liquid component containing 2 wt% HPMC was not.

Nokhodchi et al. [19] examined the different ways HPMC powder could absorb water. In this study, HPMC was in a solid state and it was hypothesized that the particles were separated spheres. Initially, the particles absorbed water molecules on the surfaces and formed a monomolecular layer resulting in an increase in the Van der Waals forces. The layers then smoothed out the surface micro-irregularities and reduced the inter-particle separation, which led to the formation of a matrix between HPMC particles and water.

As was previously discussed, the effect of HPMC on the properties of CPC was similar to the effect of citric acid (incorporated with chitosan). As the content of HPMC in the liquid component increased, the setting time decreased.

4.2 Effects of citric acid and HPMC compressive strength of the cements

Citric acid molecules were the primary components of the matrix and the water-reducing effect of citric acid improved particle packing; i.e. the particles were arranged more tightly. Hence, the porosity of the cements was reduced. Reduced porosity was previously used as a

method to improve the mechanical properties of cements [20]. Therefore, as the citric acid concentration was increased so were the mechanical properties. This was the reason why the compressive strength of G40 was better than that of G20. Especially, the post-setting SEM (Fig. 3) of A20 composition exhibited incoherent particles, so the compressive strength of this composition after setting was low.

According to the post-setting XRD profiles, hardly any HAp peaks appeared. chitosan, citric acid and HPMC did not stimulate the conversion of HAp during the setting time of the cements. Citric acid and HPMC only affected the mechanical strength of the cements through the formation of chitosan-citrate and HPMC complexes. Furthermore, although the strength value of C40 after 14 days of incubation was the highest, the transformation to HAp was less than the strength values of C20 and A20 (Fig. 5).

The transformation of TTCP and DCPD to HAp, or partial CSD to HAp through incubation caused an increase in the compressive strength of the cements. In order for HAp crystals to precipitate, the solution had to be supersaturated [15]. It was previously shown that the hydration of citric acid decreased the number of free water molecules in the liquid component. This lack of water led to the precipitation of TTCP, DCPD, and CSD, which was achieved earlier than supersaturation. These previous findings were directly applicable to the results attained in this study. In the regards to the compressive strength of G20 and G40 in terms of HPMC content, the strength value of G40 was always higher than the strength value of G20 at all incubation times. However, transformation to HAp from the initial setting 0–3 days of incubation eventually occurred. Hence, the compressive strength during this period increased in both groups (Fig. 7).

As shown in the SEM images TTCP particles adopted type I morphologies under both conditions. The morphology of A20 continually became tighter up to 14 days of incubation. In addition, the boundary particles in C20 and C40 became smoother. These changes in morphology in addition to the XRD profiles after 14 days of incubation, demonstrated that HAp conversion was initiated at the particle surface.

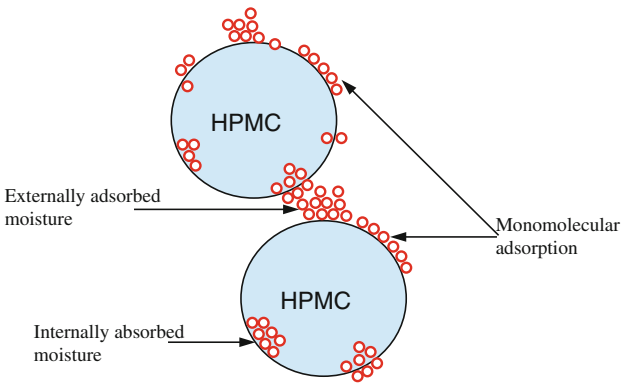

Fig. 7 Diagram of the different states of moisture

5 Conclusions

In this study, we investigated the effects of citric acid and HPMC on IBS properties. Citric acid obviously affected the setting time of the cements. When citric acid was increased, the setting time decreased. When the proportion of citric acid was fixed, the HPMC content also affected the setting time of the cements, in a similar manner as was observed for citric acid. Both citric acid and HPMC did not facilitate apatite formation immediately after the cements were set. After 14 days of incubation, the 20 wt% citric acid facilitated apatite formation better than the other compositions. However, chelation reactions between citric acid and chitosan (and HPMC) increased the compressive strength of the cements in a concentration dependent manner. The compressive strengths of the C20 and C40 compositions were the highest of each group; the values were 19.63 MPa and 23.23 (mean values), respectively. Fine fibrous structures were observed in the micro morphology of C20 and C40 after 14 days in incubation, which were not observed after setting. The micron sized fibrous structures observed in the C40 composition after setting disappeared after 14 days of incubation. The combined results of this study clearly demonstrate that HPMC and citric acid increase the CS of cements.

References

1. Yokoyama A, Yamamoto S, Kawasaki T, Kohgo T, Nakasu M. Development of calcium phosphate cement using chitosan and citric acid for bone substitute materials. Biomater. 2002;23:1091–101.
2. De Maeyer EAP, Verbeeck RMH, Vercruysse CWJ. Conversion of octacalcium phosphate in calcium phosphate cements. J Biomed Mater Res. Part A. 2000;52:95–106.
3. Sargin Y, Kizilyalli M, Telli C, Güler H. A new method for the solid-state synthesis of tetracalcium phosphate, a dental cement: X-ray diffraction and IR studies. J Eur Ceram Soc. 1997;17:963–70.
4. Vallet-Regí M, González-Calbet JM. Calcium phosphates as substitution of bone tissues. Prog Solid State Chem. 2004;32:1–31.
5. LeGeros RZ, LeGeros JP. Calcium phosphate bioceramics: past, present and future. Key Eng Mater Vols. 2003;240–242:3–10.
6. Bohner M. New hydraulic cements based on α-tricalcium phosphate/calcium sulfate dehydrate mixtures. Biomaterials. 2004;25:714–49.

7. Song HY, Esfakur Rahman AHM, Lee BT. Fabrication of calcium phosphate-calcium sulfate injectable bone substitute using chitosan and citric acid. J Mater Sci Mater Med. 2009;20:935–41.
8. Yamaguchi I, Iizuka S, Osaka A, Monmad H, Tanaka J. The effect of citric acid addition on chitosan/hydroxyapatite composites. Colloids and surf. A. Physicochem Eng Aspects 2003;214:111–8.
9. Zhang Y, Zhang M. Synthesis and characterization of macroporous chitosan/calcium phosphate composite scaffolds for tissue engineering. J Biomed Mater Res. 2001;55:304–12.
10. Zhang Y, Zhang M. Synthesis and characterization of macroporous chitosan/calcium phosphate composite scaffolds for tissue engineering. J Biomed Mater Res. 1997;35:273–7.
11. Cherng A, Takagi S, Chow LC. Effects of hydroxy propyl methylcellulose and other gelling agents on the handling properties of calcium phosphate cement. J Biomed Mater Res. 2001; 55:304–12.
12. Blouin S, Moreau MF, Weiss P, Daculsi G, Baslé MF, Chappard D. Evaluation of an injectable bone substitute (β-TCP/hydroxyapatite/hydroxyl-propyl-methyl-cellulose) in severely osteopenic and aged rats. J Biomed Mater Res Part A. 2006;78A:570–80.
13. Guo D, Xu K, Han Y. Influence of cooling modes on purity of solid-state synthesized tetracalcium phosphate. Mater Sci Eng B. 2005;116:175–81.
14. Burguera EF, Guitian F, Chow LC. Effect of the calcium to phosphate ratio on the properties of calcium phosphate bone cement. J Biomed Mater Res Part A. 2008;85A:674–83.
15. ISO 9917-1, 2003. Dentistry-water-based cements—part 1: powder/liquid acid-based cements, ISO, Geneva, Switzerland.
16. Sarda S, Fernández E, Nilsson M, Balcells M, Planell JA. Kinetic study of citric acid influence on calcium phosphate bone cements as water-reducing agent. J Biomed Mater Res. 2002;61:653–9.
17. Liu H, Li H, Cheng W, Yang Y, Zhu M, Zhou C. Novel injectable calcium phosphate/chitosan composites for bone substitute materials. Acta Biomateriallia. 2006;2:557–65.
18. Dorozhkin SV. Is there a chemical interaction between calcium phosphates and hydroxy propyl methyl cellulose (HPMC) in organic/inorganic composites? J Biomed Mater Res. 2001;54: 247–55.
19. Nokhodchi A, Ford JL, Rubinstein MH. Studies on the interaction between water and (hydroxy propyl) methyl cellulose. J Pharm Sci. 1997;86:608–15.
20. Barralet JE, Hofmann M, Grover LM, Gbureck U. High-strength apatitic cement by modification with α-hydroxy acid salts. Adv Mater. 2003;15:2091–4.